Supporting information for:

Substituent effects of auxiliary ligand in mononuclear dibenzoylmethane Dy^{III}/Er^{III} complexes: Single-molecule magnetic behavior and luminescence properties

Shan-Shan Liu,*[a] Bin Liu,[a] Man-Man Ding,[d] Yin-Shan Meng,[bc] Jia-Hui Jing,[a] Yi-Quan Zhang*[d], Xincheng Wang[a], Shijing Lin[a]

[a]Beijing Key Laboratory of Fuels Cleaning and Advanced Catalytic Emission Reduction Technology, College of Chemical Engineering, Beijing Institute of Petrochemical Technology, Beijing 102617, P. R. China.
Email: liushanshan2015@bipt.edu.cn
[b]State Key Laboratory of Fine Chemicals, Dalian University of Technology, Dalian, 2 Linggong Rd., Dalian 116024, P. R. China
[c]Beijing National Laboratory for Molecular Sciences, Beijing Key Laboratory for Magnetoelectric Materials and Devices, College of Chemistry and Molecular Engineering, Peking University, Beijing, 100871, R. P. China.
[d]Jiangsu Key Laboratory for NSLSCS, School of Physical Science and Technology, Nanjing Normal University, Nanjing 210023, P. R. China.
Email: zhangyiquan@njnu.edu.cn

Scheme S1. The structures of Hdbm, dmbipy and dmobipy

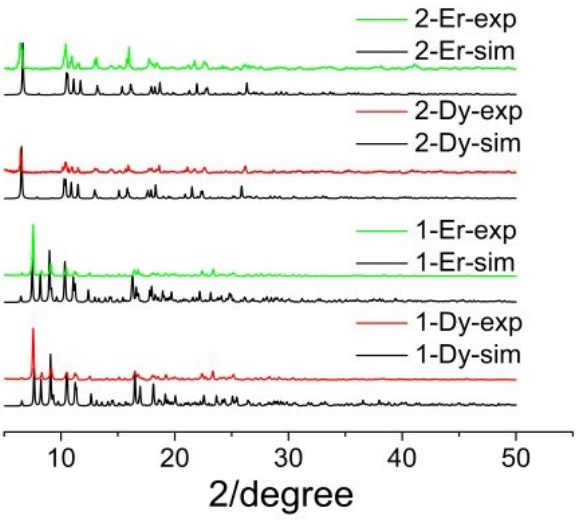

Fig. S1 Powder X-ray diffraction data of **1-Dy**, **1-Er**, **2-Dy** and **2-Er**.

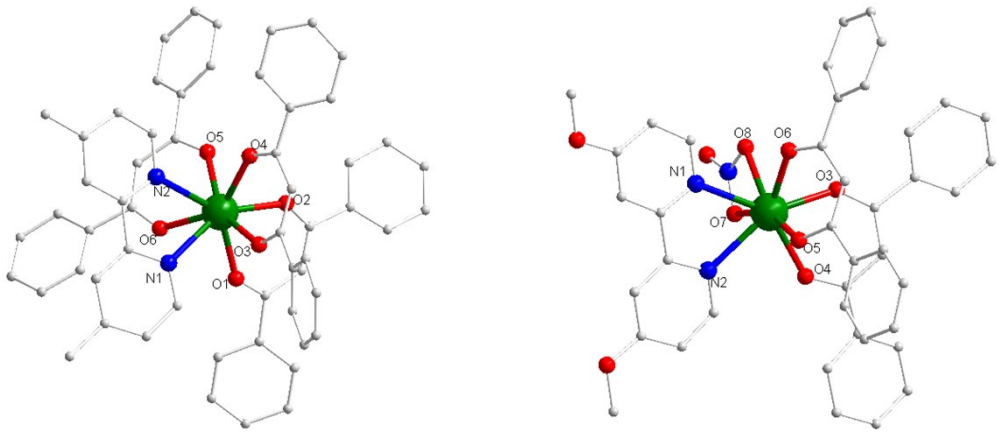

Fig. S2 The structure of **1-Er** (a) and **2-Er** (b). Color code: Er(Green), O(Red), N(Blue), C(Gray). Hydrogen atoms are omitted for clarity.

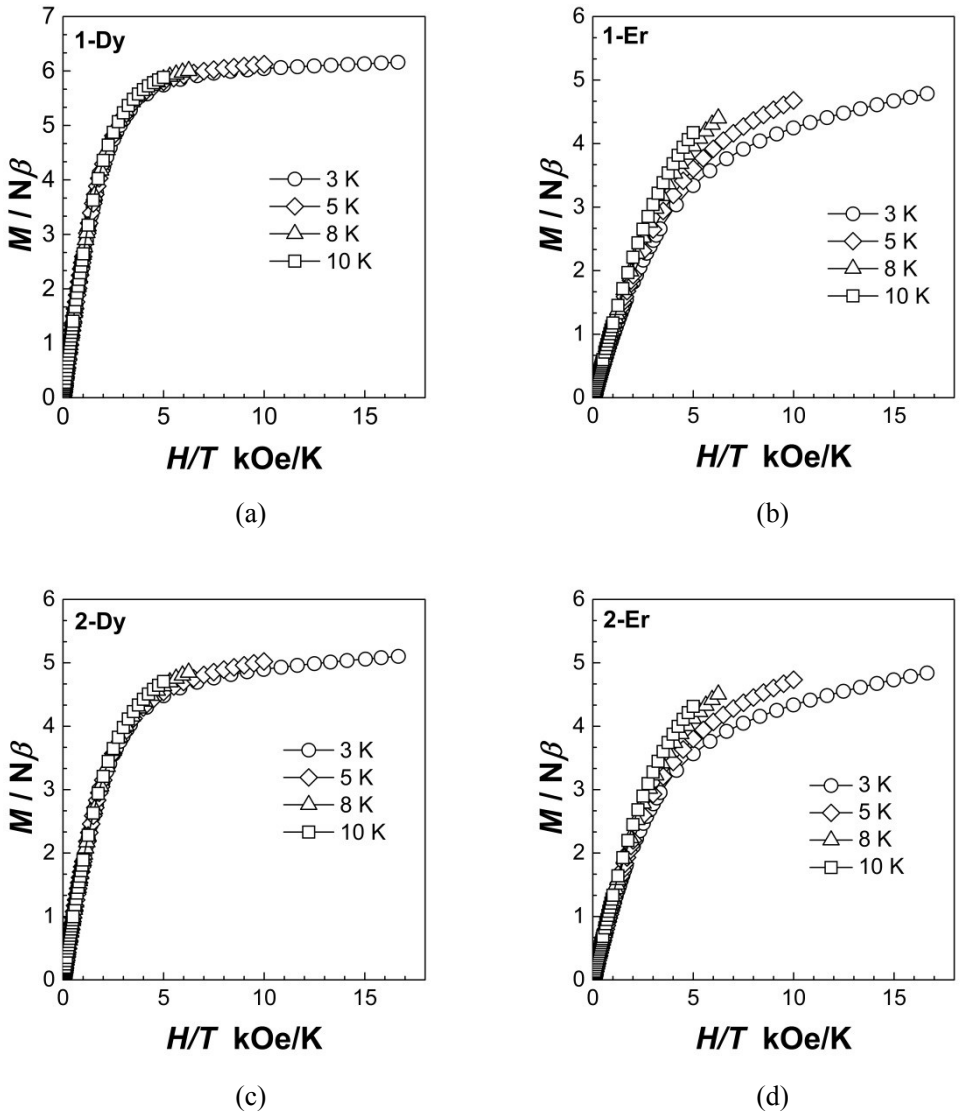

Fig. S3 $M(HT^{-1})$ curves of **1-Dy** (a), **1-Er** (b), **2-Dy** (c) and **2-Er** (d).

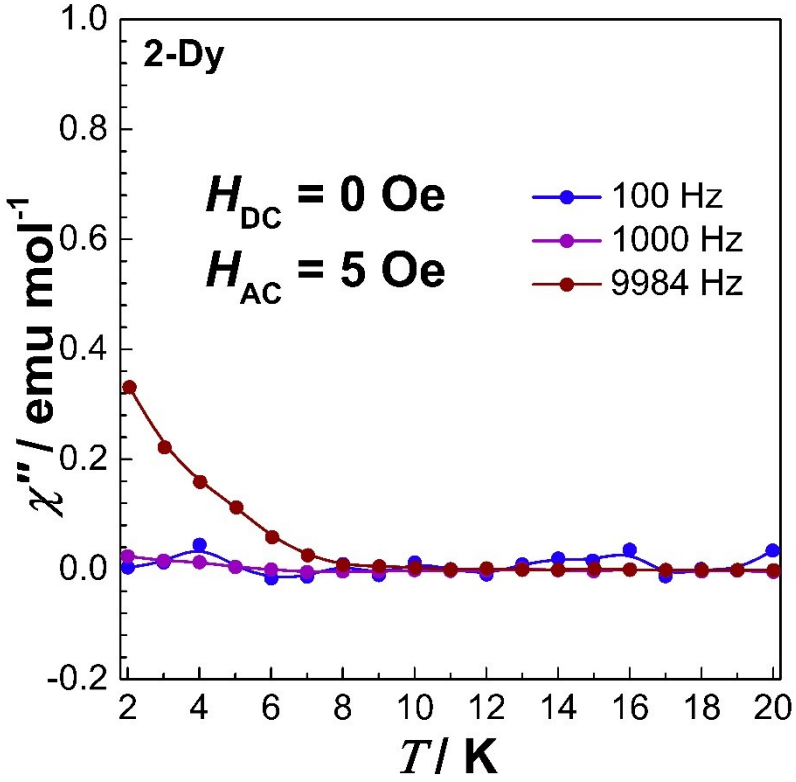

Fig. S4 Plots of χ″ ac susceptibility versus temperature of **2-Dy** under 0 dc field

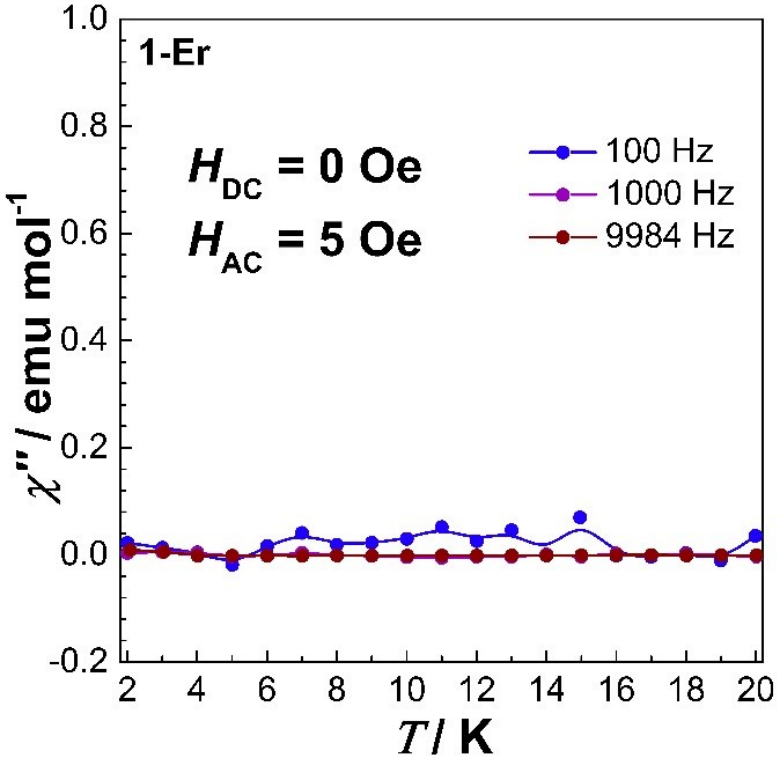

Fig. S5 Plots of χ″ ac susceptibility versus temperature of **1-Er** under 0 dc field

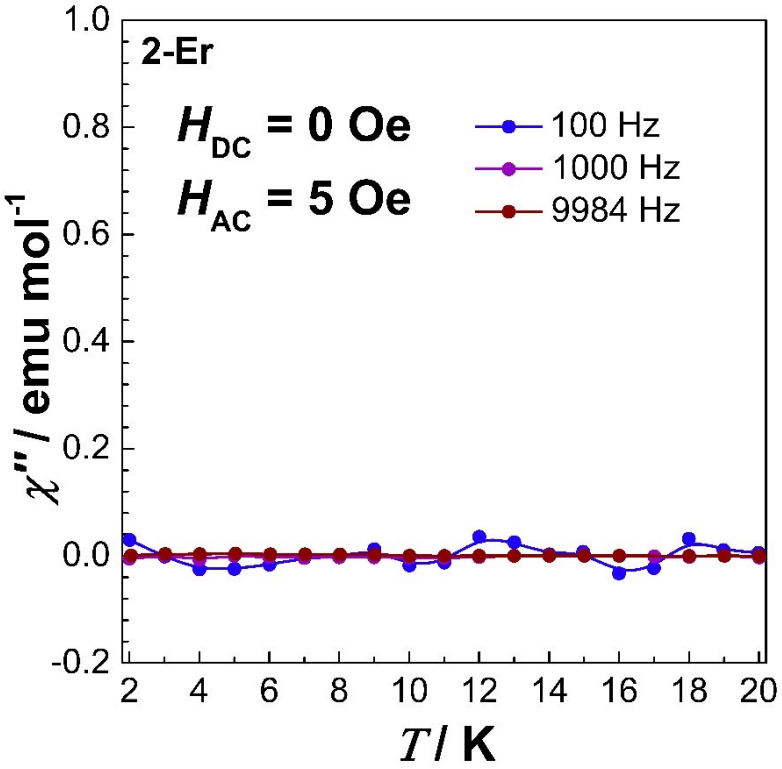

Fig. S6 Plots of χ″ ac susceptibility versus temperature of **2-Er** under 0 dc field

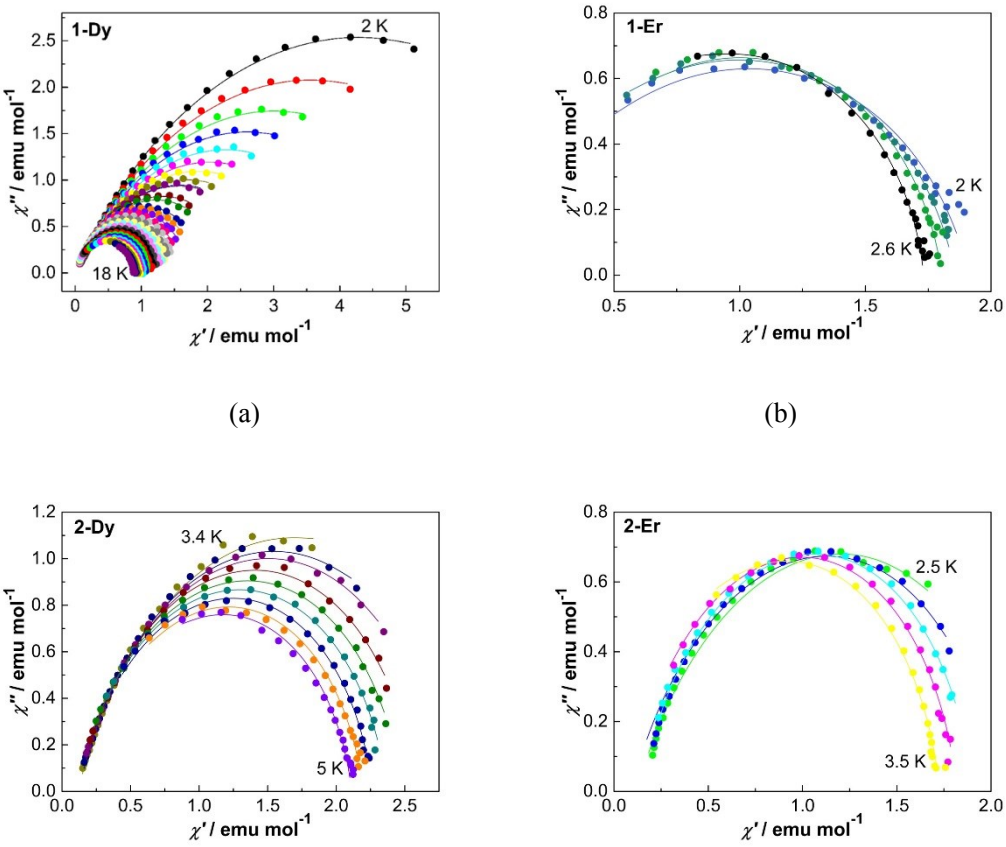

Fig. S7 Cole-Cole plots for **1-Dy** under 0 dc field (a) and **1-Er** (b), **2-Dy** (c), **2-Er** (d) under 2 kOe dc field. α values are 0.10–0.28 (**1-Dy**), 0.10–0.23(**1-Er**), 0.16–0.19 (**2-Dy**) and 0.16–0.24 (**2-Er**), respectively.

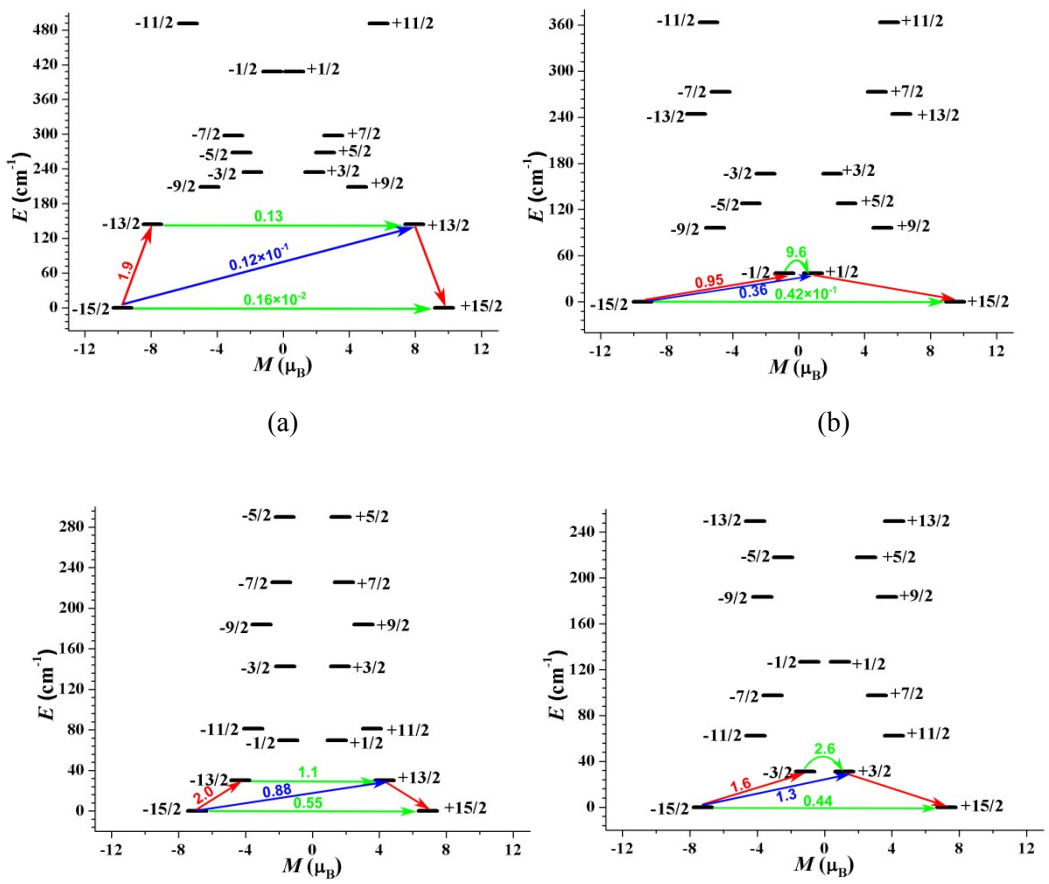

Fig. S8 Magnetization blocking barriers for **1-Dy** (a), **1-Er** (b), **2-Dy** (c) and **2-Er** (d). The thick black lines represent the KDs as a function of their magnetic moment along the magnetic axis. The green lines correspond to diagonal matrix element of the transversal magnetic moment; the blue line represent Orbach relaxation processes. The path shown by the red arrows represents the most probable path for magnetic relaxation in the corresponding compounds.

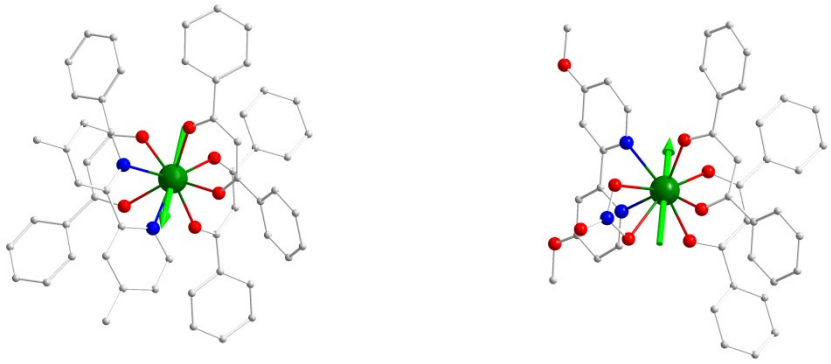

(a) (b)

Fig. S9 Orientations of the local magnetic axes on Er^{III} ions in the ground spin-orbit states for **1-Er** (a) and **2-Er** (b).

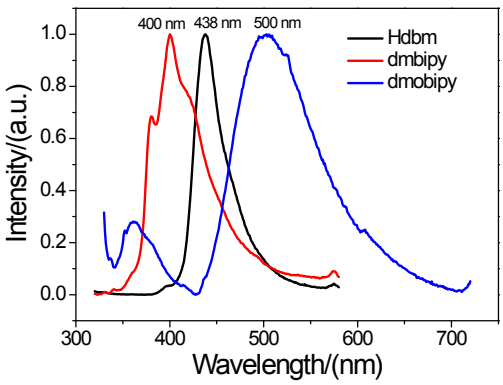

Fig. S10 Solid-state emission spectra of Hdbm, dmbipy and dmobipy.

Table S1 Crystal data and structure refinement for complexes **1-Dy**, **1-Er**, **2-Dy** and **2-Er**.

Complex	**1-Dy**	**1-Er**	**2-Dy**	**2-Er**
Formula	$C_{57}H_{45}DyN_2O_6$	$C_{57}H_{45}ErN_2O_6$	$C_{42}H_{34}DyN_3O_9$	$C_{42}H_{34}ErN_3O_9$
fw	1016.45	1021.21	887.22	891.98
Crystal system	Monoclinic	Monoclinic	Monoclinic	Monoclinic
Space group	$P2_1/n$	$P2_1/n$	$P2_1/n$	$P2_1/n$
a, Å	12.3320(3)	12.4741(11)	10.23070(10)	10.4163(11)
b, Å	23.1470(5)	23.658(2)	21.9678(2)	21.9688(19)
c, Å	16.8143(4)	16.9381(15)	16.5575(2)	16.7477(15)
α, °	90	90	90	90
β, °	100.087(2)	99.710(2)	93.8020(10)	94.344(2)
γ, °	90	90	90	90
V, Å^3	4725.43(19)	4927.0(8)	3713.04(7)	3821.4(6)
Z	4	4	4	4
T, K	180(10)	298(2)	179.99(10)	298(2)
F(000)	2060	2068	1780	1788
μ, mm^{-1}	1.635	1.755	11.285	2.256
λ, Å	0.71073	0.71073	1.54184	0.71073
R_1[a] [$I \geq 2\sigma(I)$]	0.0340	0.0536	0.0433	0.0609
wR_2[a] (all data)	0.0966	0.1047	0.1085	0.1422
S[a]	1.091	1.008	1.056	1.060

[a] Definitions: $R_1 = \Sigma ||F_o| - |F_c|| / \Sigma |F_o|$, $wR_2 = [\Sigma [w(F_o^2 - F_c^2)^2] / \Sigma [w(F_o^2)^2]]^{1/2}$, $S = [\Sigma [w(Fo^2 - Fc^2)^2]/(n-p)]^{1/2}$.

Table S2 Selected bond lengths (Å) and angles (°) for complexes **1-Dy**, **1-Er**, **2-Dy** and **2-Er**.

	1-Dy	**1-Er**	**2-Dy**	**2-Er**
Ln(1)-O(1)	2.303(2)	2.296(4)	-	-
Ln(1)-O(2)	2.341(2)	2.322(4)	-	-
Ln(1)-O(3)	2.338(2)	2.331(4)	2.284(3)	2.278(5)
Ln(1)-O(4)	2.336(2)	2.339(4)	2.339(3)	2.327(5)
Ln(1)-O(5)	2.307(2)	2.308(4)	2.261(3)	2.247(6)
Ln(1)-O(6)	2.3284(19)	2.326(4)	2.289(3)	2.278(5)
Ln(1)-O(7)	-	-	2.470(3)	2.453(6)
Ln(1)-O(8)	-	-	2.501(3)	2.495(6)
Ln(1)-N(1)	2.562(3)	2.580(5)	2.532 (3)	2.522(6)
Ln(1)-N(2)	2.569(2)	2.547(6)	2.532(3)	2.532(6)
O(1)-Ln(1)-O(2)	73.80(7)	74.11(15)	-	-
O(3)-Ln(1)-O(4)	72.15(7)	72.87(14)	72.46(9)	73.03(18)
O(5)-Ln(1)-O(6)	72.53(7)	73.03(14)	74.20(9)	75.0(2)
O(7)-Ln(1)-O(8)	-	-	51.32(9)	51.8(2)
N(1)-Ln(1)-N(2)	62.38(8)	62.94(19)	63.75(10)	64.5(2)

Table S3 Comparison of **1-Dy** and [Dy(dbm)$_3$L] complexes.

complex	Geometrical configuration	Dy…Dy distances(Å)	Dy−O (Å)	Dy−N (Å)	U_{eff}/K (H_{dc}/Oe)	Ref
[Dy(dbm)$_3$(dmbipy)]	Square antiprism	9.922	2.326	2.566	271	This work
[Dy(dbm)$_3$(bipy)]	Square antiprism	-	2.325	2.570	16.5	1
[Dy(dbm)$_3$(phen)]·Tol	Square antiprism	-	2.314	2.593	32.2	1
			2.320	2.588		
[Dy(dbm)$_3$(dpq)]·Tol	Square antiprism	-	2.320	2.574	32.1/50.6	1
	Dodecahedra		2.327	2.581	(2000)	
[Dy(dbm)$_3$(dppz)]	Square antiprism	-	2.319	2.578	27.3	1
	Bicapped trigonalprism		2.318	2.596		

(bipy = 2,2'-bipyridine, phen = 1,10-phenanthroline, dpq = dipyrazine[2,3-f:2’,3’-h]quinoxaline, dppz = dipyrido[3,2-a:2’,3’-c]phenazine, Tol = toluene)

Table S4 Wave functions with definite projection of the total moment | m_J > for the lowest two spin-orbit states for four complexes using CASSCF/RASSI-SO with MOLCAS 8.4[2].

	E/cm^{-1}	wave functions
1-Dy	0.0	93.16%|±15/2>+5.77%|±11/2>
	144.0	78.03%|±13/2>+15.95%|±9/2>
2-Dy	0.0	88.74%|±15/2>+11.96%|±11/2>
	37.3	44.11%|±1/2>+31.85%|±3/2>+14.88%|±5/2>
1-Er	0.0	68.77%|±5>+16.90%|0>+7.58%|±2>
	30.1	14.19%|±6>+23.19%|±4>+39.24%|±1>+14.76%|0>
2-Er	0.0	50.58%|±15/2>+12.19%|±13/2>+22.51%|±11/2>
	31.1	10.37%|±15/2>+10.58%|±7/2>+18.31%|±3/2>+34.95%|±1/2>

Reference

1. Y. Dong, P. Yan, X. Zou and G. Li, *Inorg. Chem. Front.*, 2015, **2**, 827–836.
2. F. Aquilante, J. Autschbach, R. K. Carlson, L. F. Chibotaru, M. G. Delcey, L. De Vico, I. Fdez. Galván, N. Ferré, L. M. Frutos, L. Gagliardi, M. Garavelli, A. Giussani, C. E. Hoyer, G. Li Manni, H. Lischka, D. Ma, P. Å. Malmqvist, T. Müller, A. Nenov, M. Olivucci, T. B. Pedersen, D. Peng, F. Plasser, B. Pritchard, M. Reiher, I. Rivalta, I. Schapiro, J. Segarra‐Martí, M. Stenrup, D. G. Truhlar, L. Ungur, A. Valentini, S. Vancoillie, V. Veryazov, V. P. Vysotskiy, O. Weingart, F. Zapata and R. Lindh, *J. Comput. Chem.*, 2016, **37**, 506-541.